

# Quasi-static test on a half-scale two-story urm building: mechanical characterization of materials

## Ensaio quasi-estático num edifício em escala reduzida (1:2) de alvenaria não armada: caracterização mecânica dos materiais

**Abide Aşikoğlu<sup>1</sup> | Alessandro Del Re<sup>2</sup> | Graça Vasconcelos<sup>3</sup> | Paulo B. Lourenço<sup>4</sup>**

<sup>1</sup> University of Minho, ISISE, Department of Civil Engineering, Guimarães Portugal, [abideasikoglu@hotmail.com](mailto:abideasikoglu@hotmail.com)

<sup>2</sup> Ecolab S.R.L., Milan, Italy, [delre.alessandro@libero.it](mailto:delre.alessandro@libero.it)

<sup>3</sup> University of Minho, ISISE, Department of Civil Engineering, Guimarães Portugal, [graca@civil.uminho.pt](mailto:graca@civil.uminho.pt)

<sup>4</sup> University of Minho, ISISE, Department of Civil Engineering, Guimarães Portugal, [pbl@civil.uminho.pt](mailto:pbl@civil.uminho.pt)

### abstract

The present paper focuses on experimental campaign of an unreinforced masonry building which represents the modern typology with concrete slabs, meaning that the structure ensures rigid diaphragm action. Accordingly, the paper is composed of two parts; (i) material characterization tests of masonry units and wallets through uniaxial, diagonal compression, and flexural tests on masonry wallets; (ii) design phase of the quasi-static test setup. The paper presents the key parameters that influenced decision-making of the design phase and general details of the test setup.

**Keywords:** Clay brick, unreinforced masonry, quasi-static test, material characterization, seismic response

### resumo

O presente trabalho centra-se na campanha experimental de um edifício de alvenaria não armada com pavimentos em betão armado, o que significa que o pavimento se pode considerar como diafragma rígido. Este trabalho é composto por duas partes; (i) ensaios de caracterização de materiais de unidades e alvenaria como material compósito através de ensaios de compressão uniaxial e diagonal, e ensaios de flexão, (ii) fase de conceção da configuração do ensaio quase estático do edifício de alvenaria. O trabalho apresenta os parâmetros-chave que influenciaram a tomada de decisão na fase de conceção, assim como aspetos gerais do esquema de ensaio do edifício.

**Palavras-chave:** Tijolo de barro, alvenaria não armada, ensaio quase estático, caracterização de material, resposta sísmica

# 1- INTRODUCTION

Unreinforced masonry buildings (URM) are largely found in many countries in the world with both low and high seismicity, which justify the improvement of European and American seismic codes concerning masonry structures (Lourenço and Marques 2020). Most recently, nonlinear static procedures have been preferred to perform performance-based design approaches, particularly in the case of masonry buildings. An extensive discussion has been carried out by Aşıkoğlu et al. (2021) to what concerns the application of such procedure to masonry buildings. Further studies are required to implement more straightforward application rules. In particular, there are various strategies to apply on masonry buildings and the nonlinear static analysis are highly dependent on the numerical procedure adopted to simulate the structure (Aşıkoğlu et al. 2019; D'Altri et al. 2019; Aşıkoğlu et al. 2020b; Lourenço and Silva 2020; Silva et al. 2020). Therefore, experimental studies play crucial role in the research community in order to validate simulations, especially, when there is a large scatter in results. The present study aims at providing an experimental data both in material and structural level so as to be used in numerical simulations with more confidence and develop straightforward rules to apply such procedure in practice.

This paper addresses the experimental campaign of (i) material characterization of masonry brick units, mortar, and masonry wallets, and (ii) the quasi-static test on a half-scaled two-story URM building and prediction of the test response. The first part is related with the characterization of the key mechanical behavior of masonry materials. For this purpose, (a) uniaxial compressive tests on mortar and masonry units; (b) flexural test on mortar specimens; (c) initial shear test for mortar-unit interface; (d) uniaxial, diagonal compression, and flexural tests on masonry wallets have been performed. The second part of the experimental work deals with the quasi-static test of a half-scaled two-story URM building with structural irregularity. The main goal is to have an insight on the response of a masonry building irregular layout and its failure patterns when subjected to lateral loading. To this end, a geometry similar to the experimental model tested by Avila et al. (2018) has been selected as illustrated in fig. 1. The half-scale two-story URM building has a plan dimension of 419 cm x 368 cm with an inter-story height of 152 cm (Fig. 1(a)). Furthermore, the box-behavior will be ensured by a RC slab, which has a 10 cm thickness. Due to irregularities in plan and elevation, center of mass and center of rigidity do not coincide with each other, resulting eccentricity of 15 and 3 cm in X and Y direction, respectively. The building is composed of vertical perforated clay masonry brick units which are already available in the market. The masonry arrangement has been decided as a running bond with the interlocking of the intersecting orthogonal walls. In literature, it is observed that there are different regularity definitions among the engineering community (Aşıkoğlu et al. 2021). Even so, the structure has so-called plan irregularity in which a setback in one corner occurs. Additionally, distribution of the openings along the elevation can be identified as irregular.

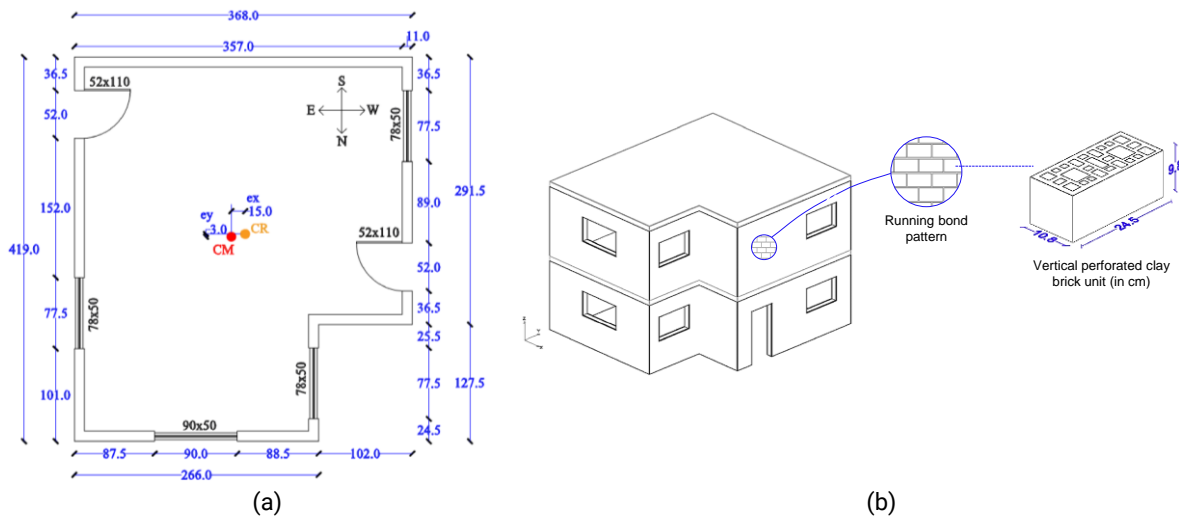


Fig. 1 | (a) Geometric details of the building plan, (b) axonometric view of the experimental building

## 2- CHARACTERIZATION OF MATERIALS

### 2.1. Unit tests

The dimensions of clay masonry brick units are 24.5 cm x 10.8 cm x 9.8 cm. As per Eurocode 6 (2018), the clay masonry material is classified as Group 3. The compressive strength of the brick units was obtained according to EN 771-1:2000 (2000). For the compression tests, three directions were considered given the anisotropic nature of the vertical perforated brick units, such as in the direction parallel to perforations (direction A), and direction perpendicular to perforations (direction B, C), as shown in Fig. 2. Six specimens were tested for each direction and the results are summarized in Table 1.



Fig. 2 | Compression test on brick units in different directions

Table 1 | Average compressive strength of brick units tested in different directions.

	Direction A	Direction B	Direction C
$F_{max}$ (kN)	231.4	18.4	126.8
$\sigma_{gross}$ (MPa)	8.7	0.7	4.8
$A_{gross}$ (mm <sup>2</sup> )	26460	10584	26460
$\sigma_{eff}$ (MPa)	15.0	3.5	9.6
$A_{eff}$ (mm <sup>2</sup> )	15428	5292	13230

Class M10 ready-mixed mortar is chosen for bed and head joints. The compressive and flexural strength of the mortar was attained according to the EN 1015-11:2007 (2007). The mortar tested was a pre-mixed M10 mortar, used for the head and bed joints. In total, 13 cubic and 7 cylindrical specimens were tested under compression, Fig. 3. The average compressive strength was obtained as 13 MPa and 8 MPa, respectively. Moreover, the average flexural strength of the mortar was attained from 7 specimens.

## 2.2. Masonry Wallet Tests

The flexural tests were designed and carried out according to BS EN 1052-2 (1999). To evaluate the flexural strength of the masonry wallets under pure bending, four-point bending tests were performed. In total, ten specimens were tested, (i) five specimens for failure parallel to the bed joints ( $f_{xkl}$ ), (ii) 5 for failure perpendicular to the bed joints ( $f_{xk2}$ ). Thus, two different geometries were considered for the masonry wallets and the details of the wallets are presented in Fig. 4. The tests were performed in displacement control at a rate of 10  $\mu\text{m/s}$ . The test equipment was assembled on a steel frame including an actuator with a capacity of 200 kN. Three LVDT's were used to measure the deformation and one LVDT was located on the hydraulic jack to control the actuator displacement. The LVDT's were located horizontally to record the flexural deformation due to the configuration of the test setup in which the specimen was placed vertically, similarly to Silva et al. (2018). The main reason is to avoid the influence of the weight of the specimen and the loading beam on the response.

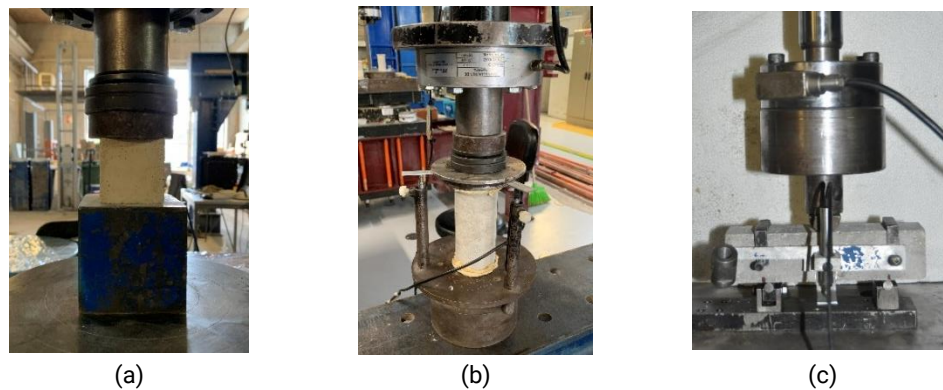


Fig. 3 | Hardened mortar tests, compression on (a) cubic, (b) cylinder samples, (c) flexural test

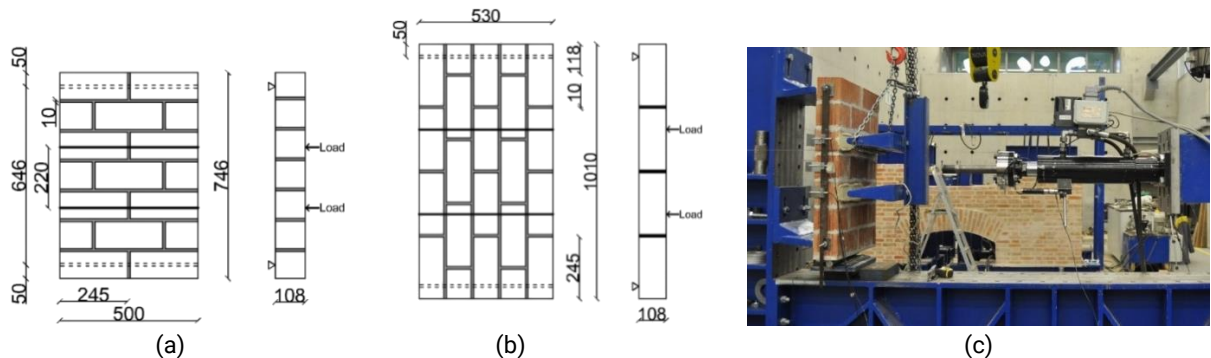


Fig. 4 | Detail of the flexural test specimens, (a) failure plane parallel to the bed joints, (b) failure plane perpendicular to the bed joints (in mm), (c) general view of four-point bending test setup for flexural tests.

The LVDT's were placed along the length of the specimen, one being in the middle of the specimens and the other two being at the loading points.

Accordingly, the flexural strength of each masonry wallet was calculated based on BS EN 1052-2 (1999) and the results are gathered in Table 2 and Fig. 5. The characteristic flexural strength parallel to the bed joint was found as 0.27 MPa, while the perpendicular counterpart was calculated as 0.51 MPa. It is noticed that the characteristic values obtained from experiments are almost 3 times and 1.25 times higher than the standard values given by Eurocode 6 (2018) for failure in parallel (0.10 MPa) and perpendicular (0.40 MPa) to the bed joint, respectively. This indicates that the standard underestimates the flexure capacity of this type of masonry.

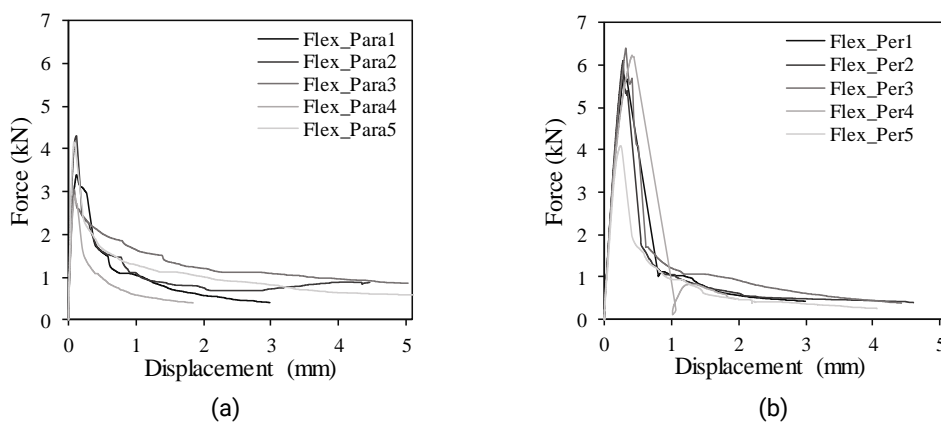


Fig. 5 | Flexural force-displacement plots, (a) failure parallel to the bed joints, (b) failure perpendicular to the bed joints

Table 2 | Mechanical properties of the masonry wallets from flexure tests

Test	Parallel to bed joint				Perpendicular to bed joint			
	$F_{max}$ (kN)	$f_{x1}$ (MPa)	$f_{x1}^{mean}$ (MPa)	$f_{xk1}$ (MPa)	$F_{max}$ (kN)	$f_{x2}$ (MPa)	$f_{x2}^{mean}$ (MPa)	$f_{xk2}$ (MPa)
1	3.39	0.38			5.77	0.77		
2	4.30	0.49			6.10	0.81		
3	3.05	0.35	0.40	0.27	6.39	0.85	0.76	0.51
4	2.92	0.33			6.23	0.83		
5	4.16	0.47			4.09	0.55		

The failure of the mortar along the parallel bed joint was generally observed in a similar pattern for all test runs as presented in Fig 6(a). Internal webs of the vertical perforated brick units appear to provide interconnection at the unit-mortar interfaces through excess mortar during the laying. To what concerns the failure perpendicular to the bed joint, the damage was noted not only along with the mortar but also along with the brick units, as shown in Fig. 6(b). The failure mechanism of the specimens in parallel to the bed joint appears to be relatively more ductile than the specimens subjected to the loading perpendicular to the bed joint because of the failure of the mortar. On the other hand, brittle behavior was observed due to the failure of the brick elements.

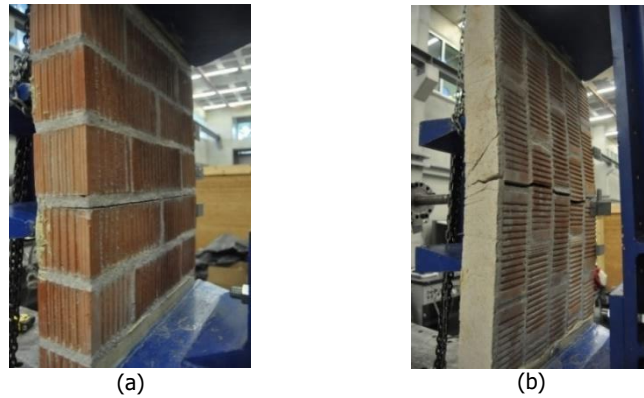


Fig. 6 | Typical failure mode, (a) parallel to the bed joint, (b) perpendicular to the bed joint

Diagonal compression tests were carried out with respect to ASTM E 519 - 02 (2002). This test method allows to determine diagonal shear or tensile strength in masonry assemblages assuming that tensile principal stress is equal to the pure shear stress state. Six specimens were constructed by considering the dimensions given by the standard and the detail of the experimental setup is given in Fig. 7. In order to apply the diagonal compression, the specimens were placed in diagonal in between steel loading shoes which were positioned opposing bottom and top corners. Uniform application of the loading was ensured by rectifying the surfaces that were in contact with the loading shoes. All specimens were tested with an actuator of 500 kN load capacity and performed under displacement control at a rate of 2 mm/s. The test was controlled by a LVDT attached to the actuator and conducted until the failure was attained. At each façade of the specimen, 2 LVDT's were instrumented to measure (i) the shortening of the vertical diagonal parallel to the applied load, (ii) the opening of the horizontal diagonal perpendicular to the applied load.

The results of the tests are presented in terms of stress-strain relation in Fig. 8(a) and the mechanical parameters are listed in Table 3. The stress-strain plots illustrate the brittle behavior of shear failure. In general, maximum force, shear stress and shear modulus slightly differ, except the fourth specimen. Although stress and maximum force observed on the first specimen has reasonable agreement with other specimens, there is a peculiar difference in the shear modulus. The reason for such discrepancy might be due to an issue related with the measurement of the transducers that could lead unreliable result for that test run. Therefore, shear modulus obtained from the first specimen was disregarded for the calculation of the mean value.

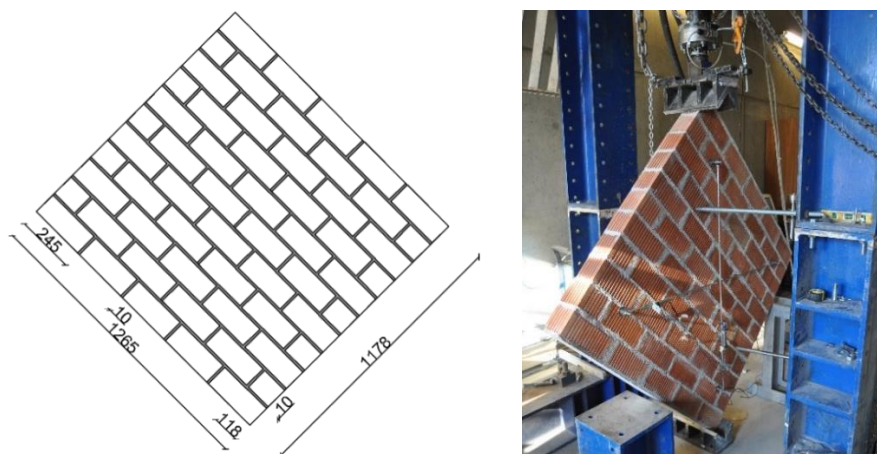


Fig. 7 | Specimen details and experimental configuration of the test (in mm)

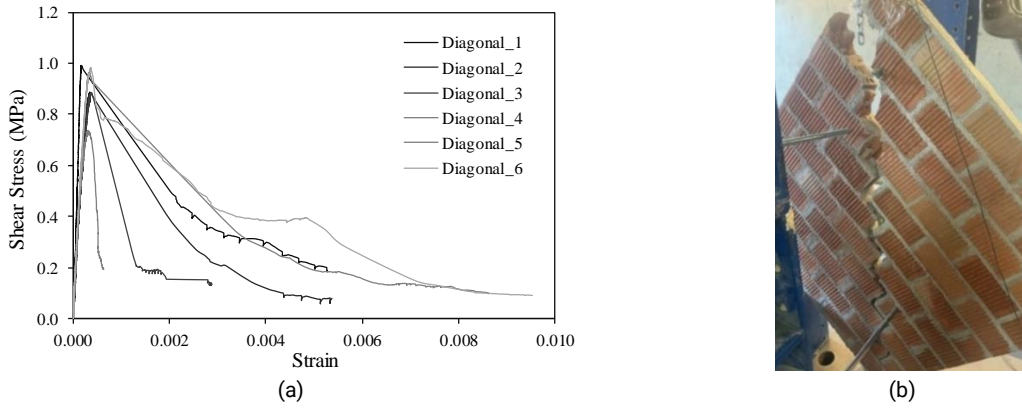


Fig. 8 | Diagonal compression test results, (a) stress-strain plot, (b) failure mode

Table 3 | Mechanical properties of the masonry wallets from diagonal compression test

Test	$F_{max}$ (kN)	$\tau_{max} = f_t$ (MPa)	G (MPa)
1	92.5	0.99	6050
2	82.7	0.89	2594
3	82.5	0.88	2309
4	68.7	0.74	2361
5	90.0	0.96	3008
6	91.7	0.98	2686
Average	84.7	0.89	2592*

\*Average value of shear modulus does not include the first test result.

It is noted that the maximum force attained at the fourth specimen was significantly lower than the other test runs. The specimen failed along the mortar bed joint of the second row of brick units. Thereupon, detachment of the mortar prevented the load flow below the crack. Under such circumstances, it is believed that the mortar bed joint which suffered from damage was the weakest link throughout the specimen. In other words, time difference due to workmanship or possible difference in the mortar mixes might influence the response. On the other hand, typical diagonal damage pattern was observed on the other specimens. Once the peak stress was achieved, the assemblages mainly collapsed in a sudden and brittle way in which stepwise crack was occurred, Fig 8(b). Consequently, the average of the diagonal shear strength and/or tensile strength of the present masonry wallets is found as 0.89 MPa while the average shear modulus is 2592 MPa.

The compressive strength of the masonry wallets was determined by performing uniaxial compression test following the standard, BS EN 1052-1 (1999). Three specimens were constructed according to the standard prescriptions. The details of the specimen and test setup are presented in Fig. 9. The test instrumentation consisted of a hydraulic actuator with a load capacity of 500 kN and five LVDT's to measure the deformation. The test was conducted under displacement control with a rate of 2 mm/s. The vertical load was applied on the top surface of the specimen to evaluate the compressive strength. For the first specimen, the load was applied with a constant increment starting from zero until the failure. However, the loading protocol was described according to the standard for other two specimens in order to determine the Young's modulus. The compressive

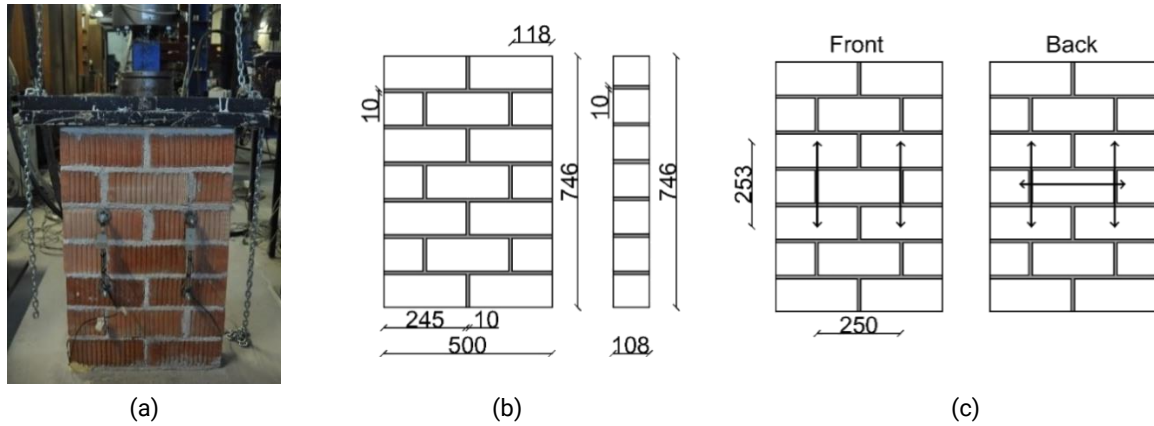


Fig. 9 | Uniaxial compression test, (a) setup, (b) geometric details, (c) LVDT configuration (in mm)

force was applied in three equal steps until the half of the maximum force that was attained from the first specimen. After each step, the compressive force kept constant for two minutes. Following to the last step, the force was increased at a constant rate until the failure. Fig. 10 illustrates the force-displacement and stress-strain relation of each specimen under uniaxial compression.

The mechanical parameters obtained from the test results are presented in Table 4. The mean compressive strength and the Young's modulus were determined as 5.7 MPa and 17518 MPa, respectively. Furthermore, the characteristic value of the masonry compressive strength is determined according to relation given by Eurocode 6 (2018) and, therefore, the minimum value is selected as resultant. In this context, the characteristic compressive strength obtained from the experimental campaign is 4.75 MPa. Additionally, the characteristic compressive strength and Young's modulus were calculated according to Eurocode 6 (2018) and given in Table 4. It is noted that compressive strength of the masonry unit and the mortar obtained from the experiments were taken account. Thus, it is possible to check the reliability of the uniaxial compression test results through the standard prescriptions. It is found that the experimental value is significantly higher (61%) than the values calculated based on the relation given in Eurocode 6 (2018).

Table 4 | Mechanical properties of the masonry assemblages under uniaxial compression

Test	$\sigma_c$ (MPa)	$f_{ck}$ (MPa)	E (MPa)	$f_{ck,EC6}$ (MPa)	$E_{EC6}$ (MPa)
1	5.2	4.33	14129		
2	6.3	5.25	23362	6.7	6700
3	5.6	4.67	15062		
Average	5.7	4.75	17518		

All panels demonstrated brittle collapse in an explosive manner. Mainly, visual cracks appeared to occur along the head joints and propagated through the brick units, as depicted in Fig. 10. In general, the failure was governed by diagonal cracks which recognized as sand clock type shape. Yet, cracking and crushing especially at the bottom corner of the panels, as well as splitting of the shells and webs were observed at the end of the test. What concerns the damage propagation, it is believed that cracking initiated on the webs of the brick units due to the fact that a set of cracking noise was noticed in the first place.

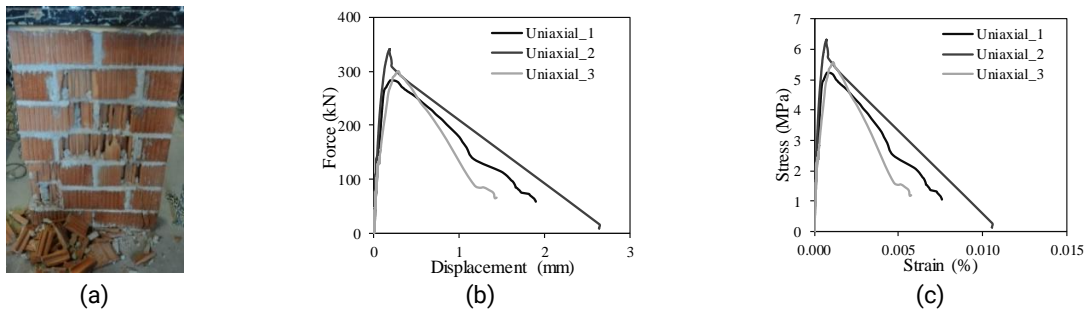


Fig. 10 | Uniaxial compression behaviour of the wallets, (a) failure mode, (b) force - displacement, (c) stress - strain curves

Initial shear strength of the unit-mortar interfaces was obtained by performing triplet test based on BS EN 1052-3 (2002). According to the standard, three different stress levels with a value of 0.2 MPa, 0.6 MPa and 1.0 MPa were used since the compressive strength of the masonry units was higher than 10 MPa. For each precompression level, three specimens were tested. In total, 5 LVDT's were used, one of them was used to control the actuator displacement while other 4 were placed at the two façades of the specimen as shown in Fig. 11. Vertical LVDT's measured relative displacement with respect to the center of the course and a horizontal LVDT was used in order to record any opening between the units that could happen. The shear force was applied under displacement control at a rate of 10 mm/s while precompression was applied by using a manual hydraulic jack.

The deformation of the specimens was measured by means of LVDT's and given in Fig 12 (a). For each specimen, shear strength ( $f_{voi}$ ) and precompression stress ( $f_{pi}$ ), and characteristic initial shear strength (or cohesion) were calculated. Moreover, correlation of the maximum shear strength and pre-compressive stress is illustrated in Fig 12(b). Definition of the linear regression of the points allows to obtain (i) initial shear strength under zero precompression ( $f_{v0}$ ) which is the interception of the obtained line with zero precompression stress, (ii) friction coefficient ( $\mu_0$ ) which is the slope of the obtained line, (iii) internal friction coefficient ( $\alpha_0$ ) which is the angle of the obtained line, and their characteristic values ( $\mu_k, \alpha_k = 0.8 \tan \alpha_0$ ).

Briefly, shear properties of the unit-mortar interface obtained from the tests are listed in Table 5. The characteristic initial shear strength is found as 0.23 MPa which is nearly 33% less than the standard value (0.30 MPa) given by Eurocode 6 (2018). The specimens showed two types of failure mode which is defined in BS EN 1052-3 (2002). It was observed that the failure mode was governed by the level of precompression. For instance, the specimens, which were tested with the lowest precompression level (0.20 MPa), presented shear failure along the mortar-unit interface while the failure under higher level of precompression was observed as splitting in the brick units.



Fig. 11 | Configuration of the test setup for initial shear test and the details of the specimen (in mm)

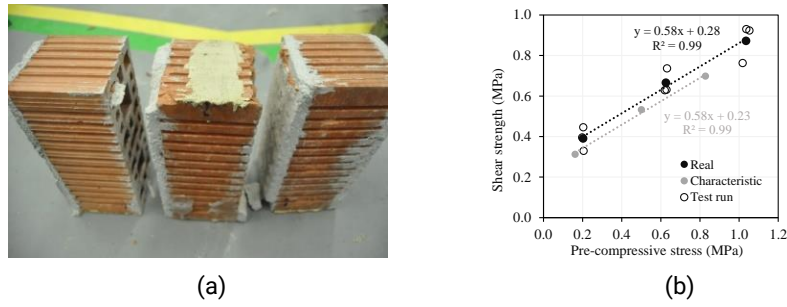


Fig. 12 | (a) Failure mode, (b) relation between maximum shear strength and pre-compressive stress

Table 5 | Mechanical properties from initial shear test

	PreComp_0.2	PreComp_0.6	PreComp_1.0
A (mm <sup>2</sup> )	26460	26460	26460
F <sub>i,max</sub> (kN)	4.9	15.1	24.9
f <sub>pi</sub> (MPa)	0.2	0.6	1.0
F <sub>max,i</sub> (kN)	18.8	32.0	41.9
f <sub>voi</sub> (MPa)	0.35	0.60	0.79
f <sub>vo</sub> (MPa)		0.28	
f <sub>vok</sub> (MPa)		0.23	
μ <sub>o</sub>		0.58	
μ <sub>k</sub>		0.58	
α <sub>o</sub> (°)		30.1	
α <sub>k</sub> (°)		30.1	

### 3- DESIGN OF THE EXPERIMENTAL SETUP

In this section, designing and planning procedure of the half-scale quasi-static test is addressed. Since the experimental campaign has not been started yet, a preliminary planning and key parameters that influenced the decision-making of experimental design is delivered, as depicted in Fig. 13. Preliminary numerical analysis allows to predict the response of the building and design and decide the components of the experiment. For instance, based on the analysis carried out by (Aşıkoğlu et al. 2020a) and (Aşıkoğlu et al. 2020b), a hydraulic actuator with a capacity of 300 kN at each level would be enough. Indeed, the hydraulic jacks is planned to be located along the axis of the center of mass to represent better the dynamic actions that activates the mass of the structure. However, it is decided to implement tube profiles along the perimeter of the building in order to avoid concentration of the load at one point (Fig. 13 (a)). Furthermore, once building is subjected to residual damage, i.e., inelastic range, it is necessary to safeguard its adjustment at the reference (zero) point during the reloading phases. In this sense, several prestressed bars will be implemented with a spacing of 75 cm along the length and width of the structure, as shown in Fig. 13 (a). These prestressed bars will be embedded in the RC slab, and they will be fixed to loading and reloading plates via load distribution profiles.

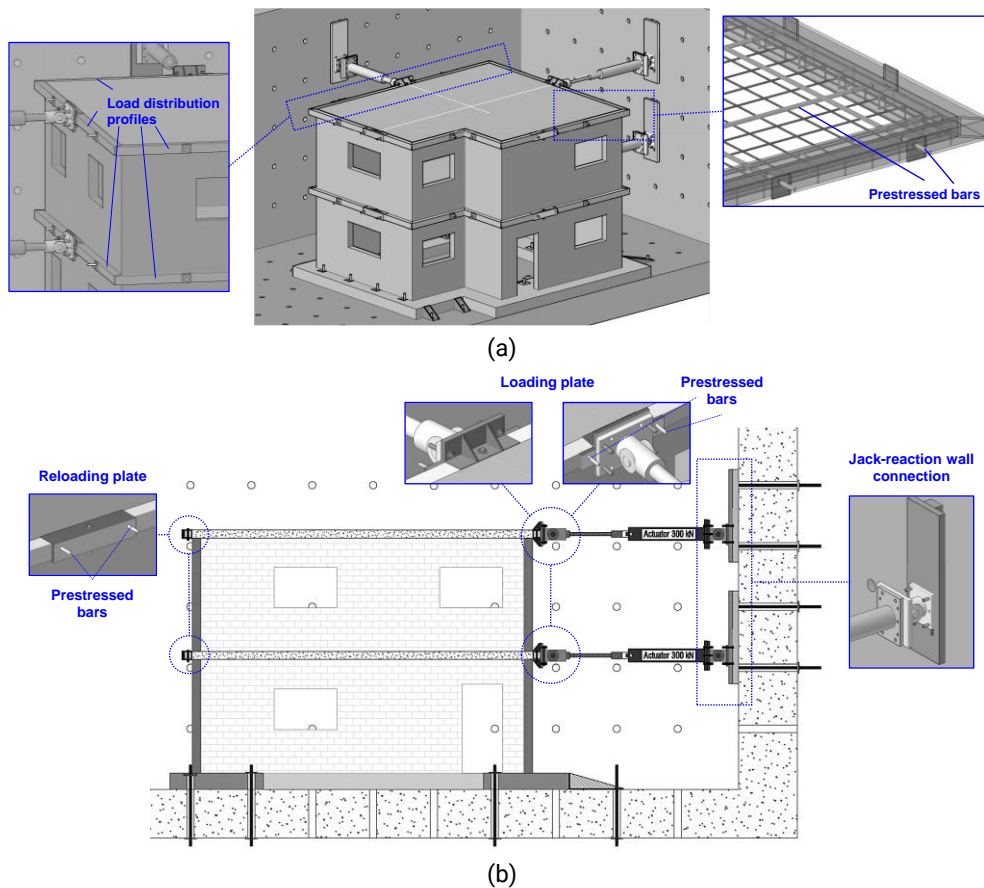


Fig. 13 | Configuration and details of the experimental setup, (a) 3D view, (b) section view

## 4- CONCLUSIONS

The present experimental work aims at studying the seismic response of a URM building with plan irregularity by performing quasi-static loading in each direction of the building. Material characterization tests have been performed to obtain the mechanical properties of the construction materials and will be further used to simulate the quasi-static test in numerical environment. Furthermore, detailed explanations on the designing experimental setup of quasi-static test are addressed. Once the experimental results are available, the numerical model will be updated to simulate the response and to derive straightforward steps to apply pushover analysis on masonry buildings.

## ACKNOWLEDGEMENTS

The first author acknowledges the financial support from the Portuguese Foundation for Science and Technology (FCT) through the Ph.D. Grant SFRH/BD/143949/2019. This work was financed by national funds through FCT - National Foundation for Science and Technology, I.P., in the scope of the research project “Experimental and Numerical Pushover Analysis of Masonry Buildings (PUMA)” (PTDC/ECI-EGC/29010/2017).

## REFERENCES

- Aşıkoğlu A, Avşar Ö, Lourenço PB, Silva LC (2019) Effectiveness of seismic retrofitting of a historical masonry structure: Kütahya Kurşunlu Mosque, Turkey. *Bull Earthq Eng* 17:3365–3395. <https://doi.org/10.1007/s10518-019-00603-6>
- Aşıkoğlu A, Vasconcelos G, Lourenço PB (2021) Overview on the Nonlinear Static Procedures and Performance-Based Approach on Modern Unreinforced Masonry Buildings with Structural Irregularity. *Buildings* 11:. <https://doi.org/10.3390/buildings11040147>
- Aşıkoğlu A, Vasconcelos G, Lourenço PB, Del Re A (2020a) Seismic response of an unreinforced masonry building with structural irregularity; Blind prediction by means of pushover analysis. In: *Brick and Block Masonry - From Historical to Sustainable Masonry*, 1st edn. CRC Press, pp 1037–1045
- Aşıkoğlu A, Vasconcelos G, Lourenço PB, Pantò B (2020b) Pushover analysis of unreinforced irregular masonry buildings: Lessons from different modeling approaches. *Eng Struct* 218:. <https://doi.org/10.1016/j.engstruct.2020.110830>
- ASTM E 519 - 02 (2002) Standard Test Method for Diagonal Tension (Shear) in Masonry Assemblages
- Avila L, Vasconcelos G, Lourenço PB (2018) Experimental seismic performance assessment of asymmetric masonry buildings. *Eng Struct* 155:298–314. <https://doi.org/10.1016/j.engstruct.2017.10.059>
- BS EN 1052-1 (1999) Methods of test for masonry - Part 1: Determination of compressive strength. European Committee for Standardization (CEN)
- BS EN 1052-2 (1999) Methods of test for masonry - Part 2: Determination of flexural strength. Eur Comm Stand
- BS EN 1052-3 (2002) Methods of test for masonry - Part 3: Determination of initial shear strength. European Committee for Standardization (CEN). Eur Comm Stand
- D'Altri AM, Sarhosis V, Milani G, et al (2019) A review of numerical models for masonry structures. Elsevier Ltd
- EN 1015-11:2007 (2007) EN 1015-11:2007 Flexural and compressive strength of mortar
- EN 771-1:2000 (2000) EN 772-1:2000 Compressive strength for masonry units
- Eurocode 6 (2018) Eurocode 6 - Design of masonry structures - Part 1-1: General rules for reinforced and unreinforced masonry structures
- Lourenço P., Marques R (2020) Design of masonry structures (General rules): Highlights of the new European masonry code. In: Kubica, Kwiecien, Bednarz (eds) *Brick and Block Masonry - From Historical to Sustainable Masonry*. Taylor & Francis, Krakow
- Lourenço PB, Silva LC (2020) Computational applications in masonry structures: From the meso-scale to the super-large/super-complex. *Int J Multiscale Comput Eng* 18:1–30. <https://doi.org/10.1615/IntJMultCompEng.2020030889>

Silva LC, Lourenço PB, Milani G (2020) Numerical homogenization-based seismic assessment of an English-bond masonry prototype: structural level application. *Earthq Eng Struct Dyn* 1–22. <https://doi.org/10.1002/eqe.3267>

Silva LM, Vasconcelos G, Lourenço P. (2018) Characterization of Materials and Masonry Assemblages for Seismic Resistant Masonry Infills. In: *Proceedings of the 1st Iberic Conference on Theoretical and Experimental Mechanics and Materials / 11th National Congress on Experimental Mechanics*. Porto, pp 781–796